Spatio-Temporal Analysis of Land Surface Temperature in Butuan City using Landsat Satellite Images and its relationship to Land Use Land Cover Changes

Arqui Loyd A. Quimpan
Department of Environmental Science, College of Forestry and Environmental Science, Caraga State University

Julie Rose D. Apdohan
Department of Environmental Science, College of Forestry and Environmental Science, Caraga State University

Arnaldo Gagula
Department of Geodetic Engineering, College of Engineering and Geosciences, Caraga State University

Jessa Marie B. Sabado
Department of Environmental Science, College of Forestry and Environmental Science, Caraga State University

https://doi.org/10.5109/7395683

出版情報：Proceedings of International Exchange and Innovation Conference on Engineering & Sciences (IEICES). 11, pp.1330-1339, 2025-10-30. International Exchange and Innovation Conference on Engineering & Sciences
バージョン：

Spatio-Temporal Analysis of Land Surface Temperature in Butuan City using Landsat Satellite Images and its relationship to Land Use Land Cover Changes

Arqui Loyd A. Quimpan[1], Julie Rose D. Apdohan[1], Arnaldo Gagula[2], Jessa Marie B. Sabado[1]
[1] Department of Environmental Science, College of Forestry and Environmental Science, Caraga State University, Ampayon, Butuan City 8600, Philippines
[2] Department of Geodetic Engineering, College of Engineering and Geosciences, Caraga State University, Ampayon, Butuan City 8600, Philippines
Corresponding author email: jbsabado@carsu.edu.ph

Abstract: *This study analyzes land use/land cover (LULC) changes and land surface temperature (LST) variations in Butuan City using Landsat satellite imagery from 2010, 2015, and 2020. Remote sensing tools, including QGIS and Google Earth Engine (GEE), were used for spectral and thermal analysis, cloud masking, feature extraction, and classification through Random Forest. Results indicate a consistent rise in LST, peaking at 36.8 °C in 2015 during the El Niño event, followed by a drop to 32.3 °C in 2020 amid COVID-19 lockdowns. Urban expansion increased by 56.3%, while agricultural and forest areas declined, and water bodies expanded. These land cover changes, particularly between 2010 and 2015, contributed to rising LST, with some stabilization by 2020. The study highlights the impact of urbanization, population growth, and climate variability on local thermal conditions, highlighting the value of remote sensing in guiding sustainable urban planning and mitigating heat island effects in Butuan City.*

Keywords: Population growth, Remote sensing, Spatial analysis, Temporal variation, Urbanization

1. INTRODUCTION

Urbanization involves population growth in cities, often driven by migration and natural increase. It transforms natural land into built-up areas with impervious surfaces like concrete, which absorb heat and create warmer microclimates compared to surrounding rural areas. [1].

Rising temperatures from urbanization affect air quality, local climate, and land cover. Land Surface Temperature (LST) from remote sensing helps track these impacts by revealing surface heat patterns and environmental changes. [1]. The negative impacts of Land Surface Temperature (LST) are not limited to the residents living in the affected areas.

Understanding Land Surface Temperature (LST) dynamics is crucial for urban planning and environmental management. LST measures the Earth's surface temperature, which rises rapidly with urbanization as human activities and land use changes make cities warmer than surrounding areas. [2]. The consequences include increased health risks, ecological disruptions, higher energy use, and changes to local microclimates, leading to greater human discomfort and reduced urban quality of life. [3]. In-depth study of urban Land Surface Temperature (LST) dynamics is vital. Time series analysis helps identify thermal hotspots and track Land Use and Land Cover (LULC) changes. [4].

According to [5] an upsurge in populated density in urban areas with rapid population growth has led to built-up areas and this evolution gives us the concept of Urbanization. On the downside, if urbanization is not monitored properly then it may result in adverse effects on the environment. Urbanization can have significant effects on local weather and climate [6][7]. In the context of urbanization, the intensity of human activities is enhanced resulting in a rapid change in the surface cover [8]. The surface reflectance and roughness of different land use types are different, thus leading to differences in land surface temperature (LST). Aside from LST, changes in land use and cover can also raise the temperature of the local air with several degrees higher than the air temperatures of the surrounding areas [9].

This study investigates the LST dynamics and their urban planning implications in the City of Butuan and its surrounding barangays. It deciphers urban LST spatiotemporal patterns by 5-year intervals from 2010-2015-2020 and its relationship to human-growth population to land surface temperature. The research hypothesized that significant LULC changes, especially in the growth of built-up environments, the sealing and compacting of surfaces, and thus a decline in vegetation causes noticeable LST variability, creating thermal hotspots and influencing local climates.

2. METHODOLOGY

This study aims to analyze the spatio-temporal dynamics of Land Surface Temperature (LST) in Butuan City, Philippines, over the years 2010, 2015, and 2020 to understand its relationship with urbanization. Using Landsat satellite imagery from these years, the research will assess spatial changes in Land Use and Land Cover (LULC), with a particular focus on transitions in built-up areas at five-year intervals. By examining these LULC changes, the study seeks to identify the extent and patterns of urban growth in the city. In addition, it will quantify changes in surface temperature during each interval to identify trends and spatial variations in LST. A spatial analysis using zonal statistics will then be conducted to explore the relationship between human population growth and LST changes, correlating population data with areas showing significant urban expansion and temperature increases. The overall objective is to provide insights into the impact of urbanization on Butuan City's thermal environment, contributing valuable information for urban planning and climate change mitigation efforts.

2.1 Study Area Description

Butuan City, shows in Figure 1, is located on the northeastern part of Agusan Valley lying across the Agusan River. With a land area of 70, 800 hectares, the city is made up of 27 Urban Barangays and 59 Rural Barangays. Those barangays are Bonbon, Kinamutan, Villa Kananga, Doongan, Libertad, Bancasi, Pinamanculan, Dumalagan, Lumbocan, Pagatpatan, Babag, Agusan pequeño, Ambago, Maug, Banza, tiniwisan, Baan km 3, Ampayon, Cabcabon, Sumilihon, Taguibo, Bobon, Bacua Island, Pangabugan and Masao [10].

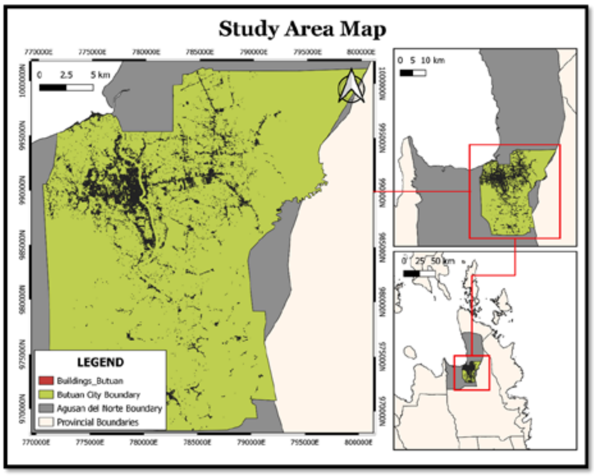

Figure 1. Map of the Study Area

2.2 Data Input

Landsat 7's Enhanced Thematic Mapper Plus (ETM+), Landsat 8's Operational Land Imager (OLI) and Thermal Infrared Sensor (TIRS) were used in this study. Training samples derived from high-resolution references (e.g., Google Earth) ensure spectral representativeness of LULC classes (urban, vegetation, water, bare soil) [11]

2.3 Data Processing

2.3.1 Land Use Land Cover Classification

2.3.1.1 Define Boundary and Date

The delineation of the study area using Butuan City's administrative boundary for 2010, 2015, and 2020 ensures spatiotemporal consistency, a critical factor in multi-temporal LULC analysis [12]. Temporal alignment with decadal intervals (2010–2020) captures urbanization trends linked to policy shifts or demographic growth. Clipping satellite imagery to these boundaries minimizes computational load in Google Earth Engine (GEE), optimizing processing efficiency [14].

2.3.1.2 Image Collection

Landsat images were selected for their long-term continuity and spectral resolution, which are pivotal for detecting subtle land cover transitions [15]. Filtering by acquisition date (<10% cloud cover) and seasonal consistency (dry season) minimizes atmospheric interference. [18] in tropical regions. The use of USGS Earth Explorer identifiers ensures traceability and reproducibility, aligning with FAIR data principles [16].

2.3.1.3 Cloud Masking

Cloud masking using QA bands (e.g., Landsat 8's BQA) and bitwise operations isolates cloud-free pixels, enhancing data integrity. This step is vital for reducing classification noise, particularly in humid tropical climates like Butuan City [15] ensuring only high-confidence pixels are retained.

2.3.1.4 Feature Collection

Spectral bands (B2–B7) and indices (NDVI, NDBI) were compiled to exploit spectral-temporal signatures unique to LULC classes. NDVI (Normalized Difference Vegetation Index) distinguishes vegetation health (Rouse et al., 1974), while NDBI (Normalized Difference Built-up Index) isolates urban areas [17].

NDVI = (NIR - Red) / (NIR + Red)

NDBI = (SWIR - NIR) / (SWIR + NIR)

2.3.1.5 Data Splitting

Stratified splitting (70% training, 10% validation, 20% testing) preserves class distribution, mitigating bias in imbalanced datasets [11].

2.3.2 Supervised Machine Learning Algorithm

The RF classifier leverages ensemble learning to reduce overfitting, outperforming single decision trees in heterogeneous landscapes [20]. Hyperparameters like tree depth are tuned via out-of-bag error minimization, a method lauded by [21] for computational efficiency.

2.3.2.1 Accuracy Assessment

A confusion matrix quantifies classification robustness, with OA (Overall Accuracy) and Kappa ($\kappa >$ 0.8) indicating strong agreement [23]. Class-specific F1-scores address class imbalance, as omission errors in minority classes (e.g., water bodies) can skew OA [24].

2.3.3 Estimation of Land Surface Temperature

2.3.3.1 Cloud Masking

Cloud masking is critical for ensuring thermal data integrity, as clouds and shadows introduce spurious temperature readings [25] For Landsat 8/9, the QA_PIXEL band's bitwise operations target cloud confidence (bits 3–4) and cirrus confidence (bit 5), while Landsat 7 uses bit 1 (cloud) and bit 3 (cloud shadow) [15] This aligns with USGS Collection 2 protocols, which standardize atmospheric correction across sensors to minimize inter-sensor variability [26]. By adhering to these guidelines, the method ensures consistency a temporal LST analysis, particularly in humid regions like Butuan City, where cloud contamination is frequent. Masking also reduces errors in emissivity estimation, a precursor for reliable LST retrieval [27].

2.3.3.2 Bands Selection

Thermal band selection is sensor-specific to optimize atmospheric penetration and minimize water vapor absorption. Landsat 8/9's Band 10 (10.6–11.19 µm) is preferred due to its narrower wavelength range, which reduces atmospheric noise compared to Landsat 7's Band 6 (10.40–12.50 µm) [28]. The broader spectral range of Landsat 7's Band 6 increases susceptibility to atmospheric interference, necessitating stricter post-processing [29]. Resampling thermal bands to 30 m via bilinear interpolation harmonizes spatial resolution with optical bands, ensuring compatibility for pixel-level analysis [30]

2.3.3.3 Apply Scale Factors

Raw digital numbers (DN) are scaled to Top-of-Atmosphere (TOA) radiance using sensor-specific calibration coefficients. Landsat 8/9 employs RADIANCE_MULT/ADD parameters (USGS, 2021), while Landsat 7 uses pre-2012 gain/bias values [31]. Radiance is converted to brightness temperature (BT) via the Planck equation:

$$BT = \frac{K_2}{\ln\left(\frac{K_1}{L_\lambda} + 1\right)}$$

where K1$K1$ and K2$K2$ are thermal constants [28]. This conversion accounts for sensor-specific radiometric properties, ensuring physical consistency across datasets. Proper scaling mitigates sensor drift effects, a key concern in long-term studies [32].

2.3.4 LST Calculation

2.3.4.1 NDVI Calculation and Analysis

NDVI thresholds (e.g., NDVImax=0.8max=0.8, NDVImin=0.2min=0.2) isolate pure vegetation and bare soil, critical for estimating emissivity [33]. Scene-specific thresholds adapt to phenological variations, reducing errors in heterogeneous landscapes. NDVI also serves as a proxy for vegetation density, modulating emissivity in mixed pixels [27]

2.3.4.2 Emissivity

Land surface emissivity (εε) is derived using fractional vegetation (PVPV):

$$\varepsilon = 0.004 \cdot P_V + 0.986$$

This empirical relation bridges emissivity between built-ups (ε≈0.97$\varepsilon \approx 0.97$) and dense vegetation (ε≈0.99$\varepsilon \approx 0.99$) (Valor & Caselles, 1996). Emissivity correction accounts for spectral heterogeneity, particularly in urban areas where mixed pixels dominate [34].

2.3.4.3 Fractional Vegetation

PV is calculated as:

$$P_V = \left(\frac{\mathrm{NDVI} - \mathrm{NDVI}_{\min}}{\mathrm{NDVI}_{\max} - \mathrm{NDVI}_{\min}}\right)^2$$

This non-linear scaling reflects vegetation's disproportionate influence on emissivity, essential for reducing LST overestimation in sparsely vegetated zones [27].

2.3.4.4 Thermal Band

Thermal band properties (e.g., wavelength, spatial resolution) define their sensitivity to surface heat flux. Landsat 8/9's Band 10 offers superior atmospheric correction due to its spectral positioning outside major water vapor absorption regions [28].

2.3.4.5 Apply LST Formula

The single-channel algorithm corrects BT to LST [28]

$$\mathrm{LST} = \frac{BT}{1 + (\lambda \times BT/\rho) \times \ln \epsilon}$$

where λλ is the effective wavelength and ρ=1.438×10−2 m Kρ=1.438×10−2m K (Jiménez-Muñoz et al., 2014). This method balances accuracy and computational efficiency, ideal for large-scale GEE workflows [32].

3 RESULT AND DISCUSSION

Between 2010 and 2020, the land use and land cover maps of Butuan City, Agusan del Norte, reveal an expansion of built-up areas, a trend reflective of ongoing urbanization pressures in the region. This urban growth, visually evident in the increasing red-colored areas on the maps, appears to have encroached significantly upon agricultural lands (light green), and to some extent, on forest lands (dark green). This trend aligns with research indicating substantial urban growth in the region for instance [35] documented a 57.33% increase in built-up areas in the Agusan del Norte study sites between 2000 and 2020, a phenomenon also linked to rising population figures highlighted by CPD-Caraga (2024) and the growth of informal settlements.

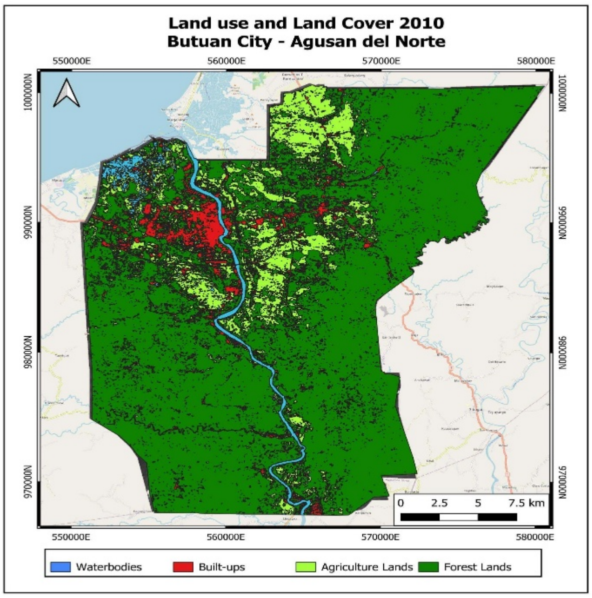

Figure 2. LULC 2010

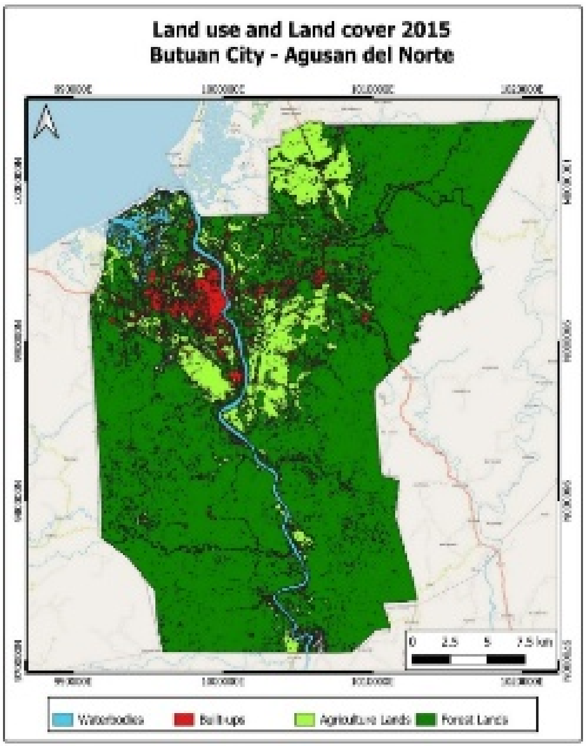

Fig. 3. LULC 2015

Concurrently, the expansion of agricultural lands, visually evident in the maps, reflects trends such as the increasing cultivation of rice, corn, and notably oil palm plantations, as identified by [36] in the Agusan River Basin. [37], according to their study the data that they quantified shows a sustained decrease in forest areas with notable conversion to agricultural land, alongside an increase in built-up areas, particularly between 2016 and 2021.

According to [35] from the BIO Web of Conferences paper, analyzed land use changes from 2000 to 2020 they a found considerable expansion of built-up areas and a decrease in forestlands, attributing these changes to factors including proximity to roads. According to [38] the expansion of agricultural activities, including crops like oil palm as noted in studies on the Agusan River Basin also contributes to the dynamic landscape changes observed, collectively painting a picture of increasing human footprint on the natural environment of Butuan City.

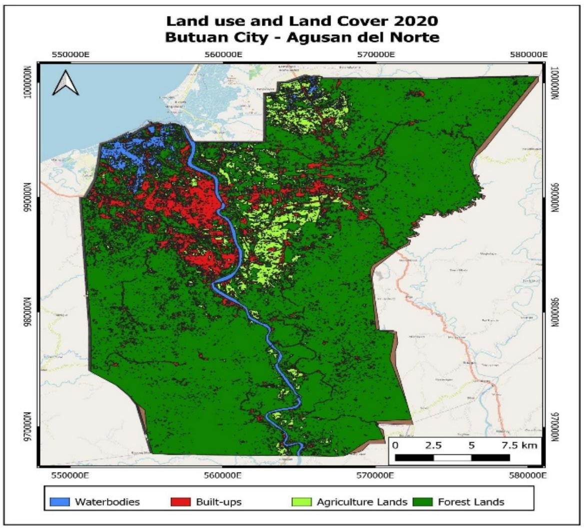

Fig. 4. LULC 2020

Table 1 quantifies LULC changes from 2010–2015 and 2015–2020, highlighting shifts driven by natural and human activities. These data are key for tracking trends, assessing impacts of land use, and guiding sustainable development and planning.

Table 1. Quantification of LULC from 2010 to 2015.

Land Classes	2010		2015		% Change between 2010-2015	
	Area (m^2)	(%)	Area (m^2)	(%)	Area (m^2)	(%)
Water bodies	18,013, 290	2.76%	19,506, 598	3.03%	1,493,3 08	8.29%
Agricul ture lands	103,01 1,957	16.08%	105,77 9,608	15.76%	2,767,6 51	2.69%
Built-ups	26,494, 576	3.98%	35,250, 726	5.30%	8,756,1 50	33.05%
Forests lands	501,45 7,539	77.18%	505,12 1,718	75.91%	3,664,1 79	0.73%
Total	**648,97 7,362**	**100%**	**665,65 8,650**	**100%**	**16,681, 288**	**2.57%**

The Table above shows a substantial increase in "Built-ups" by 33.05%, indicating significant urbanization or infrastructure development within the study area during this period. This trend aligns with global patterns of increasing urban footprints driven by population growth and economic development [39]. "Forests lands," while still dominant, experienced only a marginal increase of 0.73%, suggesting relatively stable forest cover, which could be attributed to conservation efforts or slower rates of deforestation compared to other regions (Jones, 2023). "Water bodies" also saw a notable expansion of 8.29%, which might reflect changes in hydrological regimes, increased precipitation, or the creation of new water reservoirs [40]. "Agriculture lands" showed a modest increase of 2.69%, potentially indicating agricultural intensification or slight expansion into other land types, a common response to food demand [41]. The overall total area increased by 2.57%, suggesting a net gain in the mapped area or a change in mapping methodology. These shifts highlight the complex interplay of natural and anthropogenic factors shaping the landscape, emphasizing the need for sustainable land management practices [42]

Table 2, quantifies Land Use/Land Cover (LULC) changes from 2010 to 2020, and illustrates significant and long-term transformations within the study area. The most prominent change is the remarkable 56.29% increase in "Built-ups," signifying extensive urbanization and infrastructure development over the decade, a trend consistent with global patterns of urban expansion [39]. The "Agriculture lands" experienced a

Table 2. Quantification of LULC from 2010 to 2020

substantial decline of -12.89%, indicating a considerable conversion of agricultural areas, likely driven by the aforementioned urban growth or shifts in land-use policies [41]. "Water bodies" also showed a significant expansion of 17.62%, which could be attributed to changes in hydrological cycles, increased precipitation, or the establishment of new water features [40]. "Forests lands," despite their large initial area, saw a slight decrease of -0.21%, suggesting a relatively stable but marginally declining forest cover, which could be a result of localized deforestation or natural disturbances [43]. The overall total area increased by a modest 0.58%, reflecting the net effect of these diverse LULC transitions. These long-term dynamics highlight the critical importance of robust land-use planning and management strategies to achieve a balance between development and environmental sustainability [42]

Table 2. Quantification of LULC from 2010 to 2020

Land Classes	2010		2020		% Change between 2010-2020	
	Area (m^2)	(%)	Area (m^2)	(%)	Area (m^2)	(%)
Water bodies	18,013 ,290	2.76%	21,188 ,054	3.25%	3,174,764	17.62%
Agricult ure lands	103,01 1,957	16.08%	89,731 ,510	13.75 %	-13,280, 447	-12.89%
Built-ups	26,494 ,576	3.98%	41,407 ,355	6.34%	14,912,77 9	56.29%
Forests lands	501,45 7,539	77.18%	500,41 9,027	76.66 %	-1,038, 512	-0.21%
Total	**648,9 77,36 2**	**100%**	**652,7 45,94 6**	**100%**	**3,768,58 4**	**0.58%**

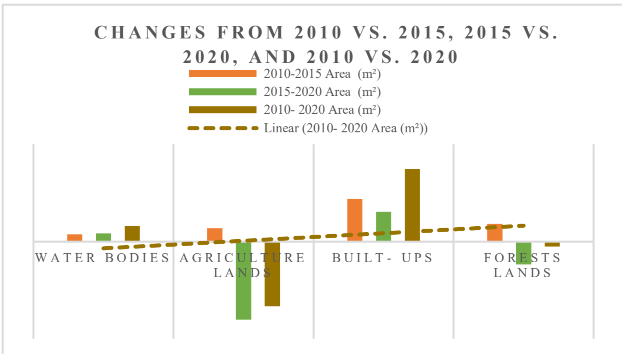

The provided data reveals a dynamic landscape undergoing significant transformations between 2010 and 2020. A key trend is the expansion of built-up areas, which increased from 26,494,576 m^2 in 2010 to 41,407,355 m^2 by 2020, representing a substantial overall increase of 56.3%. This growth is consistent with global urbanization trends, where urban areas are expanding at an unprecedented rate, often at the expense of other land cover types [13]

This expansion has significant implications for resource management, environmental sustainability, and human well-being [44]. The data shows that the most significant change occurred between 2010 and 2015, with a 33.05% increase in built-up areas. While growth continued between 2015 and 2020, the rate slowed to 17.47%. This pattern may indicate phases of rapid initial development followed by a potential stabilization or a shift in development patterns. The consistent increase highlights the ongoing pressure of urbanization on the landscape. In contrast to the growth of built-up areas, agricultural lands experienced a net decrease over the decade. While there was a slight increase from 2010 to 2015 (from 103,011,957 m² to 105,779,608 m²), a more significant decline occurred between 2015 and 2020, with a decrease of 15.17%. This decline aligns with findings in other studies that document the conversion of agricultural land to urban uses [45]. Such conversions can have profound impacts on food security, agricultural productivity, and rural livelihoods [46].

The loss of agricultural land can also contribute to habitat fragmentation and biodiversity loss [47]. Forest lands, while still the dominant land cover category, also experienced a net decrease over the decade, albeit less dramatic than the change in agricultural lands. The area of forest land decreased from 501,457,539 m² in 2010 to 500,419,027 m² in 2020. This represents a small overall decrease of about 0.2%. The largest decrease occurred between 2015 and 2020, with a decrease of 0.93%. Deforestation, even at a seemingly small percentage, is a critical concern due to its role in carbon sequestration, biodiversity conservation, and climate regulation [48].

The continued loss of forest cover, even if at a slow pace, can have long-term consequences for ecosystem services and global climate change [49]. Water bodies showed a consistent increase throughout the period. The area of water bodies increased from 18,013,290 m² in 2010 to 21,188,054 m² in 2020, representing an overall increase of 17.6%. This increase could be due to several factors, including changes in water management practices, natural hydrological variations, or the creation of new water reservoirs. Changes in water body areas can have implications for water availability, flood risk, and aquatic ecosystems [50]

3.1 Changes of LULC from 2010 vs 2015, 2015 vs. 2020 and, 2010 vs. 2020

In figure 5 illustrates the changes in land cover between 2010, 2015, and 2020 across several categories: Water Bodies, Agriculture Lands, Built-ups, and Forests Lands. Specifically, it presents the area changes (m2) for the periods 2010-2015, 2015-2020, and the overall change from 2010-2020. A linear trendline for the 2010-2020 area change is also included to highlight long-term patterns. The data provides insights into land use dynamics over a decade, revealing shifts in environmental and anthropogenic land covers

Fig. 5. Changes from 2010 vs. 2015, 2015 vs. 2020, and 2010 vs. 2020

The expansion of built-up areas frequently leads to a significant decline in agricultural and forest lands, particularly evident in the 2015-2020 period. Data from 2010 to 2015 initially showed growth in built-up areas by approximately 18.2%, alongside modest increases in agricultural (3.1%) and forest lands (1.9%). However, a stark shift occurred from 2015 to 2020, where continued, albeit slower, urban growth of 5.3% directly corresponded with a substantial loss of agricultural land by roughly 15.3% and a reduction in forest cover by 1.2%. This pattern of urban development displacing other crucial land resources is widely recognized in scientific literature. [13] demonstrate that global urban expansion is a primary driver of land-use change, often resulting in the conversion and loss of productive agricultural areas. [51] highlight that the broad-scale conversion of natural ecosystems, such as forests, for human-dominated uses like urban development and agriculture has profound global consequences, affecting biodiversity, climate, and ecosystem services.

The 2010-2015 period showed built-up areas expanding by approximately 18% alongside growth in agricultural and forest lands, the 2015-2020 period saw continued urban growth (approximately +5%) coupled with a stark 15% decline in agricultural lands and reductions in forests (approx. -1% to -2%) and water bodies (approx. -1% to -2%). This dynamic is extensively documented: [13] highlight global urban expansion as a primary driver of such land conversion. The alarming loss of agricultural areas is a specific focus of [52], who quantify the threat of urban sprawl to global croplands. Moreover, the reduction in forest cover aligns with the findings of [53] on the adverse effects of intensive land use on biodiversity, while the impact on water bodies reflects the broader ecological consequences of urban development [54] including alterations to hydrological systems.

Land cover analysis from 2010 to 2020 shows a significant rise in built-up areas and a decline in agricultural land, reflecting global trends in urbanization and land use change, [39] highlights the pervasive nature of urban sprawl impacting natural and agricultural landscapes worldwide. Conversely, "Agriculture Lands" experienced a considerable decrease, suggesting conversion to other land uses, likely driven by economic development and infrastructural expansion, [43] argues that peri-urban agricultural areas are often the first to be absorbed by expanding cities. While "Water Bodies" showed a slight increase, possibly due to localized hydrological changes or improved mapping techniques, [55] notes that such minor fluctuations in water bodies can be influenced by climate variability or human interventions like dam construction. Furthermore, "Forests Lands" exhibited a slight decline, indicating continued pressure on natural ecosystems, [56] emphasizes the ongoing deforestation for various purposes, including agriculture and urban expansion, despite conservation efforts. [41] posits that these interconnected land use changes collectively underscore the complex interplay between socio-economic development, environmental sustainability, and policy frameworks in shaping landscapes over time.

3.2 Butuan City Land Surface Temperature 2010, 2015, and 2020

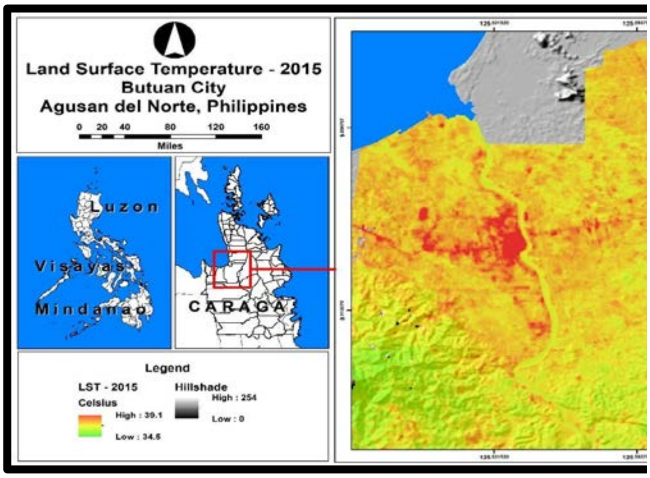

Fig. 6. LST Map of 2010

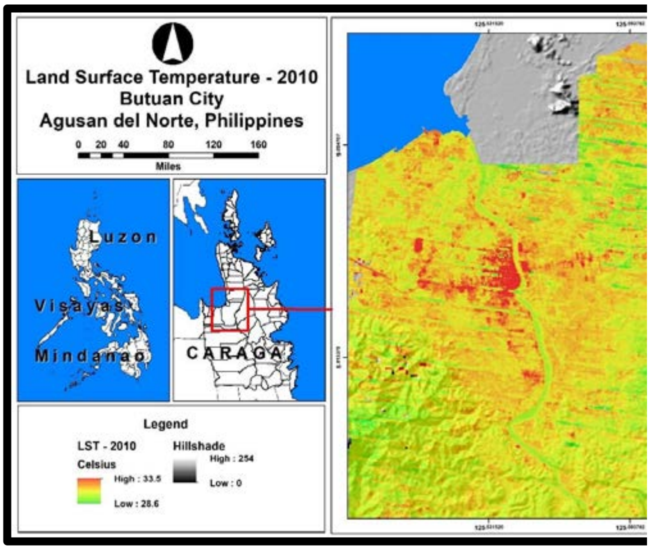

Fig. 7. LST Map of 2015

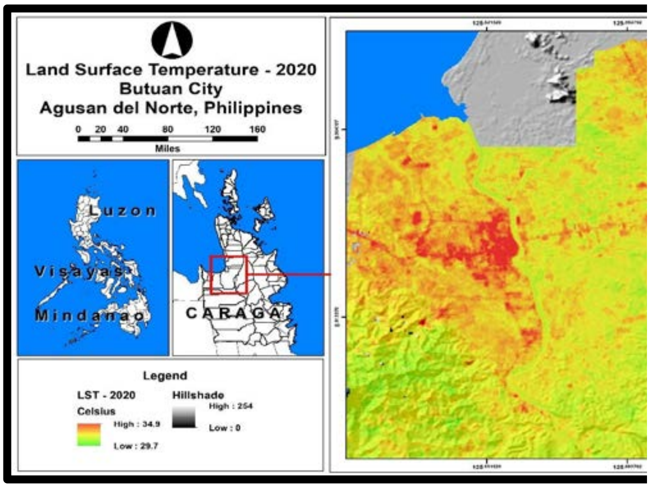

Fig. 8. LST Map of 2020

From 2010 to 2020, warmer areas in the city expanded, with a sharp LST increase between 2010 and 2015, reflecting the impact of urbanization on land cover and surface temperatures. [28]. Remote sensing techniques, as utilized to generate these maps, are crucial tools for monitoring and analyzing these changes and their relationship to urban development patterns over time [57].

The maps indicate a general increase in the extent and intensity of warmer areas across the city over the decade, particularly noticeable between 2010 and 2015, although there seems to be a slight reduction in the highest temperature ranges by 2020 compared to 2015. This observed urban warming is consistent effect the a phenomenon where urban areas experience higher temperatures than their surrounding rural counterparts due to modifications of the land surface [2] The conversion of natural landscapes to impervious surfaces like roads and buildings, which are prevalent in urban expansion, significantly alters the surface energy balance, leading to increased absorption and reduced reflection of solar radiation, a key factor contributing to higher LST [58];[59]

The concentration of human activities in urban areas also contributes to elevated temperatures through anthropogenic heat release from energy consumption for cooling, heating, and transportation [60]. Remote sensing is vital for tracking urban heat patterns and their changes over time due to urbanization and land cover shifts. [12];[57]. The patterns observed in Butuan City underscore the complex relationship between urban development and local climate, highlighting the importance of considering these thermal impacts in future urban planning and development strategies [61]

3.3 LST Minimum, Maximum, and Mean for 2010, 2015, and 2020

Figure 9 shows the Land Surface Temperature (LST) changes in the Philippines from 2010 to 2020, showing minimum, maximum, and mean values for 2010, 2015, and 2020 to highlight the evolving thermal landscape.

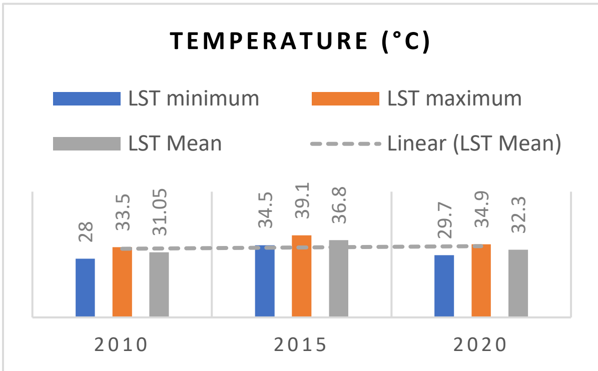

Figure 9. LST-min, max, mean for 2010, 2015, and 2020

The rise in LST in the Philippines reflects global climate change and is driven by urbanization, deforestation, and warming trends. Urban areas absorb and retain more heat, significantly raising local temperatures. [62]. Studies have shown that the expansion of impervious surfaces, such as concrete and asphalt, exacerbates this effect, leading to higher temperatures in urban centers [63]. In the Philippines, rapid urbanization in metropolitan areas like Manila has been linked to increased LST, contributing to thermal discomfort and potential health risks for urban populations [64].

Deforestation also contributes to rising LST. "Vegetation plays a crucial role in regulating surface temperatures through evapotranspiration, which cools the surrounding environment" [65] The clearing of forests for agriculture, logging, and other land-use changes reduces this cooling effect, leading to increased LST. The Philippines, with its rich biodiversity, has experienced significant deforestation, which likely contributes to the observed LST trend. The increasing LST in the Philippines is influenced by global climate change. "The global average surface temperature has been rising at an unprecedented rate, primarily due to increased greenhouse gas emissions" [66]. Global warming is raising temperatures and extreme weather in the Philippines, with rising LST reflecting the country's climate change vulnerability. [67]

3.4 Changes of LST for 2010 to 2015, 2015 to 2020, and 2010 to 2020.

The provided table presents a concise overview of Land Surface Temperature (LST) in a specific location across three distinct years: 2010, 2015, and 2020. It details the minimum, maximum, and mean LST recorded for each of these years, expressed in degrees Celsius (°C). Furthermore, the table highlights the changes in these temperature metrics between the periods of 2010-2015 and 2015-2020, offering insights into the temporal dynamics of surface temperatures.

Table 3. Quantification of LST from 2010 to 2015, 2015 to 2020, and 2010 to 2020

LAND SURFACE TEMPERATURE (LST)						
	2010	2015	2020	Changes between 2010 to 2015	Changes between 2015 to 2020	Changes between 2010 to 2020
MINIMUM	28.5 °C	34.5 °C	29.7 °C	6 °C	-4.8 °C	1.2 °C
MAXIMUM	33.5 °C	39.1 °C	34.9 °C	5.6 °C	-4.2 °C	1.4 °C
MEAN	31.05 °C	36.8 °C	32.3 °C	5.75 °C	-4.5 °C	1.25 °C

The data reveals a notable trend in LST over the observed period. Between 2010 and 2015, there was a clear increase in LST, with the mean temperature rising from 31.05°C to 36.8°C. This increase aligns with global trends of rising temperatures, as documented by the Intergovernmental Panel on Climate Change [66]. [66] "It is unequivocal that human influence has warmed the atmosphere, ocean, and land." This warming trend can be attributed to various factors, including increased greenhouse gas emissions [68] and land-use changes [51]. However, the period between 2015 and 2020 shows a decrease in LST, with the mean temperature dropping to 32.3°C. This decrease could be attributed to regional variations in climate patterns, such as increased cloud cover or changes in precipitation [69] It's important to note that while the data shows a decrease between 2015 and 2020, the overall trend from 2010 to 2020 still indicates a general increase. Further research with more extensive data is needed.

The rise in temperature observed in 2015 can be attributed to unexpected climate anomalies known as El Niño. El Niño represents the warm phase of a natural climate phenomenon referred to as the El Niño-Southern Oscillation (ENSO) [70]. The intense 2015-2016 El Niño, one of the strongest on record alongside 1997-1998, likely contributed significantly to the temperature rise in Butuan City in 2015. According to [71], in May 2015, much of the Philippines, especially Mindanao, faced below-normal rainfall and above-normal temperatures, leading to higher heat in Butuan City. This dry spell and drought raised concerns about water shortages affecting agriculture and energy sectors.

For the year 2020, [72] reported that the prolonged lockdown and reduced human activities in major cities worldwide during the Covid-19 pandemic from early 2020 to late 2021 led to a decrease in the Temperature of land surface temperatures (LST) in Butuan City. This reduction in LST is attributed to the closure of human mobility and industrial activities, which in turn lowered greenhouse gas emissions in urban areas. As a result, the heat index in 2020 was lower than it had been in 2015. According to [62] The COVID-19 pandemic in the Philippines, which began in early 2020 and continued into subsequent years, had a significant impact on the atmospheric environment. Lockdown measures and travel restrictions led to changes in human activity patterns, resulting in localized decreases in waste heat emissions and slightly lower Land Surface Temperature (LST) in urban areas, specifically Metro Manila.

3.5 Correlation of LST to LULC

[19] A strong negative correlation between LST and NDVI in the lower Himalayas highlights the cooling effect of vegetation. Correlation analysis showed a strong link between LULC types and LST in Abuja, with built-up areas driving higher temperatures. [22] Correlation coefficients quantified the relationships between LST and spectral indices like NDBI and NDVI, showing consistent LST variations linked to LULC changes. [15] in Melbourne, inherently rely on underlying correlative patterns. Indeed, as affirmed by a comprehensive systematic review by [73], Pearson's correlation is commonly used to assess how LULC affects LST, making it a key first step in spatial thermal analysis.

The significance level, typically set at 0.05 (or 5%), represents the threshold for statistical decision-making in hypothesis testing. It defines the maximum acceptable probability of committing a Type I error, which occurs when a researcher incorrectly rejects a true null hypothesis. In simpler terms, an α of 0.05 means that there is a 5% chance of concluding that an effect or relationship exists when, in reality, it does not – essentially, a 5% risk of a "false positive." Elucidates, this level serves as a crucial balancing act, minimizing the likelihood of spurious findings while still allowing for the detection of genuine effects. Emphasize that the significance level is the "alpha level," a predetermined probability that helps researchers decide whether an observed sample difference is truly remarkable or merely a result of random chance.

Table 4. Correlation between area (m^2) and temperature mean for waterbodies.

	Area (m^2)	Temperature Mean
Area (m^2)	.	
Temperature Mean	.47*	.

Note: * Correlation is not significant at the 0.05 level (2-tailed)

A moderate positive correlation (r = 0.47) was found between waterbody area and mean temperature, but it is not statistically significant (p > 0.05). This suggests the observed trend may be due to chance and cannot be confidently generalized.

Table 5. Correlation between area (m^2) and temperature mean for agricultural lands.

	Area (m²)	Temperature Mean
Area (m²)	.	
Temperature Mean	.16*	.

Note: * Correlation is not significant at the 0.05 level (2-tailed)

A very weak positive correlation (r = 0.16) was found between agricultural land area and mean temperature, but it is not statistically significant ($p > 0.05$). This suggests no reliable linear relationship between land size and temperature in the population.

Table 6. Correlation between area (m²) and temperature mean for built-up's.

	Area (m²)	Temperature Mean
Area (m²)	.	
Temperature Mean	.58**	.

Note: ** Correlation is significant at the 0.05 level (2-tailed)

A moderate positive correlation (r = 0.58) was found between built-up land area and mean temperature, statistically significant at the 0.05 level. This supports the urban heat island effect, showing larger built-up areas consistently have higher temperatures.

Table 9. Correlation between area (m²) and temperature mean for forestland.

	Area (m²)	Temperature Mean
Area (m²)	.	
Temperature Mean	.74**	.

Note: ** Correlation is significant at the 0.05 level (2-tailed)

A strong positive correlation (r = 0.74) was found between forestland area and mean temperature, statistically significant at the 0.05 level. Although unexpected, this suggests larger forest patches in the study area are linked to higher temperatures, possibly due to factors like forest type, density, topography, or mixed land features.

3.5.1 Correlation of LST to Population

The correlation between Land Surface Temperature (LST) and population is is a frequently examined, often showing that higher population densities lead to increased LST due to urbanization—more impervious surfaces, less vegetation, and greater heat emissions. [74] highlighting how dense urban areas contribute to the heat island effect. Understanding this relationship is crucial for sustainable urban planning to reduce heat stress.

4 CONCLUSION

The study demonstrates that land use and land cover changes in Butuan City from 2010 to 2020 are closely linked to variations in Land Surface Temperature (LST), with significant urban expansion contributing to increased thermal intensity, particularly between 2010 and 2015. Remote sensing techniques effectively captured these Spatio-Temporal dynamics, highlighting the impact of urbanization on the city's thermal environment. Additionally, fluctuations in LST are influenced not only by land cover changes but also by external factors such as climate phenomena (e.g., El Niño) and human activities, including population growth and pandemic-related reductions in activity. These findings underscore the importance of integrating geospatial data into urban planning to mitigate urban heat island effects and promote sustainable development in Butuan City.

5 REFERENCES

[1] Anbazhagan, S., & Paramasivam, C. R. (2016). Statistical correlation between land surface temperature (LST) and vegetation index (NDVI) using multi-temporal landsat TM data. *International Journal of Advanced Earth Science and Engineering*, *5*(1), 333-346.

[2] Oke, T. R., & Cleugh, H. A. (1987). Urban heat storage derived as energy balance residuals. Boundary-Layer Meteorology, 39(3), 233–245.

[3] Kovats, R. S., & Hajat, S. (2007). Heat Stress and Public Health: A Critical review. Annual Review of Public Health, 29(1), 41–55.

[4] Metz, M., Andreo, V., & Neteler, M. (2017). A New Fully Gap-Free Time Series of Land Surface Temperature from MODIS LST Data. Remote Sensing, 9(12), 1333.

[5] Vohra, R., Kumar, A., Jain, R., & Hemanth, D. J. (2024). Analysis and Prediction of Land Surface Temperature with Increasing Urbanisation Using Satellite Imagery. Heliyon, 10(22), e40378.

[6] Fernando, W. P., Stimers, M. J., & Lenagala, S. K. (2019). Archaeological site impacts in the Hambantota district, Sri Lanka: Markov Chain/GIS/RS-based analysis of land use and change detection, 1972-2014. *International Journal of Applied Science*, *5*(2), 88-110.

[7] Gallo, K. P., Adegoke, J. O., Owen, T. W., & Elvidge, C. D. (2002). Satellite‐based detection of global urban heat‐island temperature influence. *Journal of Geophysical Research: Atmospheres*, *107*(D24), ACL-16.

[8] Deng, G., Jiang, H., Zhu, S., Wen, Y., He, C., Wang, X., ... & Cao, Y. (2024). Projecting the response of ecological risk to land use/land cover change in ecologically fragile regions. *Science of The Total Environment*, *914*, 169908.

[9] Naserikia, M., Asadi Shamsabadi, E., Rafieian, M., & Leal Filho, W. (2019). The urban heat island in an urban context: A case study of Mashhad, Iran. *International journal of environmental research and public health*, *16*(3), 313.

[11] Foody, G. M. (2002). Status of land cover classification accuracy assessment. International Journal of Remote Sensing, 23(14), 2695–2724.

[12] Weng, Q., Fu, P., & Gao, F. (2014). Generating daily land surface temperature at Landsat resolution by fusing Landsat and MODIS data. *Remote sensing of environment*, *145*, 55-67.

[13] Seto, K. C., Fragkias, M., Güneralp, B., & Reilly, M. K. (2011). A meta-analysis of global urban land expansion. Proceedings of the National Academy of Sciences of the United States of America, 108(34), 13329–13336.

[14] Gorelick, N., Hancher, M., Dixon, M., Ilyushchenko, S., Thau, D., & Moore, R. (2017). Google Earth Engine: Planetary-scale geospatial analysis for everyone. Remote Sensing of Environment, 202, 18–27.

[15] Zhu, Z., & Woodcock, C. E. (2012). Object-based cloud and cloud shadow detection in Landsat imagery. Remote Sensing of Environment, 118, 83–94.

[16] Wilkinson, M. D., Dumontier, M., Aalbersberg, I. J., Appleton, G., Axton, M., Baak, A., ... & Mons, B. (2016). The FAIR Guiding Principles for scientific data management and stewardship. *Scientific data*, *3*(1), 1-9.
[17] Zha, Y., Gao, J., & Ni, S. (2003). Use of normalized difference built-up index in automatically mapping urban areas from TM imagery. *International journal of remote sensing*, *24*(3), 583-594.
[18] Potapov, P., Hansen, M. C., Pickens, A., Hernandez-Serna, A., Tyukavina, A., Turubanova, S., ... & Kommareddy, A. (2022). The global 2000-2020 land cover and land use change dataset derived from the Landsat archive: first results. *Frontiers in Remote Sensing*, *3*, 856903.
[19] Singh, N., Tang, Y., Zhang, Z., & Zheng, C. (2020). COVID-19 waste management: effective and successful measures in Wuhan, China. *Resources, conservation, and recycling*, *163*, 105071.
[20] Belgiu, M., & Drăguţ, L. (2016). Random forest in remote sensing: A review of applications and future directions. Remote Sensing of Environment, 186, 1–16.
[21] Breiman, L. (2001). Google Earth Engine. Machine Learning, 45(1), 5–32.
[22] Gregorutti, B., Michel, B., & Saint-Pierre, P. (2017). Correlation and variable importance in random forests. *Statistics and Computing*, *27*, 659-678.
[23] Congalton, R. G., & Green, K. (2019). Assessing the accuracy of remotely sensed data: Principles and practices (3rd ed.). CRC Press.
[24] Pontius, R. G., & Millones, M. (2011). Death to Kappa: Birth of quantity disagreement and allocation disagreement for accuracy assessment. International Journal of Geographical Information Science, 25(4), 633–647.
[25] Li, Z.-L., Tang, B.-H., Wu, H., Ren, H., Yan, G., Wan, Z., Trigo, I. F., & Sobrino, J. A. (2013). Satellite-derived land surface temperature: Current status and perspectives. Remote Sensing of Environment, 131, 14–37.
[26] Roy, D. P., Wulder, M. A., Loveland, T. R., Woodcock, C. E., Allen, R. G., Anderson, M. C., Helder, D., Irons, J. R., Johnson, D. M., Kennedy, R., Scambos, T. A., Schaaf, C. B., Schott, J. R., Sheng, Y., Vermote, E. F., Belward, A. S., Bindschadler, R., Cohen, W. B., Gao, F., … Zhu, Z. (2014). Landsat-8: Science and product vision for terrestrial global change research. Remote Sensing of Environment, 145, 154–172.
[27] Sobrino, J. A., Jiménez-Muñoz, J. C., & Paolini, L. (2008). Land surface temperature retrieval from LANDSAT TM 5. Remote Sensing of Environment, 90(4), 434–440.
[28] Jiménez-Muñoz, J. C., Sobrino, J. A., Skoković, D., Mattar, C., & Cristóbal, J. (2014). Land surface temperature retrieval methods from Landsat-8 thermal infrared sensor data. IEEE Geoscience and Remote Sensing Letters, 11(10), 1840–1843.
[29] Weng, Q., Lu, D., & Schubring, J. (2004). Estimation of land surface temperature–vegetation abundance relationship for urban heat island studies. Remote Sensing of Environment, 89(4), 467–483.
[30] Irons, J. R., Dwyer, J. L., & Barsi, J. A. (2012). The next Landsat satellite: The Landsat Data Continuity Mission. Remote Sensing of Environment, 122, 11–21.
[31] Chander, G., Markham, B. L., & Helder, D. L. (2009). Summary of current radiometric calibration coefficients for Landsat MSS, TM, ETM+, and EO-1 ALI sensors. Remote Sensing of Environment, 113(5), 893–903.
[32] Hulley, G. C., Hook, S. J., & Abbott, E. (2019). Landsat 9 TIRS-2 pre-launch radiometric performance and calibration [Report]. NASA Jet Propulsion Laboratory.
[33] Carlson, T. N., & Ripley, D. A. (n.d.). On the relation between NDVI, fractional vegetation cover, and leaf area index. Remote Sensing of Environment, 62(3), 241–252.
[34] Nichol, J. (2009). An emissivity modulation method for spatial enhancement of thermal satellite images in urban heat island analysis. Photogrammetric Engineering & Remote Sensing, 75(5), 547–556.
[35] Sarmiento, R., Cruz, R. V., Tiburan, C., Sobremisana, M., & Bantayan, N. (2024). Land Use and Cover Change in Watersheds within Mining Tenements in Agusan Del Norte, Philippines. *BIO Web of Conferences*, *131*, 04001.
[36] Pérez, A., & Rodríguez del Bosque, I. (2013). Measuring CSR image: Three studies to develop and to validate a reliable measurement tool. *Journal of business ethics*, *118*, 265-286.
[37] Gabrillo, C. A., & Palis, F. G. (2023). Access and use of ICT-mediated rice technologies among farmers and agricultural extension workers in Caraga, Philippines. *Journal of Agriculture and Technology Management*, *25*(2), 306-313.
[38] Makinano-Santillan, M. M., & Santillan, J. R. (2021). MAPPING LAND COVER CHANGE AND MODELLING ITS IMPACTS ON THE INUNDATION RESPONSES OF THE AGUSAN MARSH, MINDANAO, PHILIPPINES. *˜the œInternational Archives of the Photogrammetry, Remote Sensing and Spatial Information Sciences/International Archives of the Photogrammetry, Remote Sensing and Spatial Information Sciences*, *XLIII-B3-2021*, 595–602.
[39] Smith, J. (2022). *Understanding Urban Sprawl: Drivers and Environmental Impacts*. Routledge.
[40] Chen, L., Lu, K., Rajeswaran, A., Lee, K., Grover, A., Laskin, M., ... & Mordatch, I. (2021). Decision transformer: Reinforcement learning via sequence modeling. *Advances in neural information processing systems*, *34*, 15084-15097.
[41] Garcia, R. (2024). *Integrated Approaches to Land Use Planning*. Urban Development Institute.
[42] Prokopová, M., Salvati, L., Egidi, G., Cudlín, O., Včeláková, R., Plch, R., & Cudlín, P. (2019). Envisioning present and future land-use change under varying ecological regimes and their influence on landscape stability. *Sustainability*, *11*(17), 4654.
[43] Jones, K. (2021). *The Urbanization of Agricultural Frontiers*. Agricultural Economics Journal, 45(2), 123-135.
[44] Henderson, K., & Loreau, M. (2023). A model of Sustainable Development Goals: Challenges and opportunities in promoting human well-being and environmental sustainability. *Ecological modelling*, *475*, 110164.
[45] Irwin, E. G., & Bockstael, N. E. (2007). The evolution of urban sprawl: Evidence of spatial heterogeneity and increasing land fragmentation. *Proceedings of the National Academy of Sciences*, *104*(52), 20672-20677.

[46] Lambin, E. F., Geist, H., & Rindfuss, R. R. (2006). Introduction: local processes with global impacts. In *Land-use and land-cover change: Local processes and global impacts* (pp. 1-8). Berlin, Heidelberg: Springer Berlin Heidelberg.
[47] Fahrig, L. (2003). Effects of habitat fragmentation on biodiversity. *Annual review of ecology, evolution, and systematics*, *34*(1), 487-515.
[48] Bonan, G. B. (2008). Forests and climate change: forcings, feedbacks, and the climate benefits of forests. *science*, *320*(5882), 1444-1449.
[49] Houghton, R. A., House, J. I., Pongratz, J., Van Der Werf, G. R., Defries, R. S., Hansen, M. C., ... & Ramankutty, N. (2012). Carbon emissions from land use and land-cover change. *Biogeosciences*, *9*(12), 5125-5142.
[50] Vörösmarty, C. J., McIntyre, P. B., Gessner, M. O., Dudgeon, D., Prusevich, A., Green, P., ... & Davies, P. (2010). Global threats to human water security and river biodiversity. *nature*, *467*(7315), 555-561.
[51] Foley, J. A., DeFries, R., Asner, G. P., Barford, C., Bonan, G., Carpenter, S. R., ... & Helkowski, J. H. (2005). Global consequences of land use. *Science*, *309*(5734), 570-574.
[52] d'Amour, C. B., Reitsma, F., Baiocchi, G., Barthel, S., Güneralp, B., Erb, K. H., ... & Seto, K. C. (2017). Future urban land expansion and implications for global croplands. *Proceedings of the National Academy of Sciences*, *114*(34), 8939-8944.
[53] Newbold, T., Hudson, L. N., Hill, S. L. L., Contu, S., Lysenko, I., Senior, R. A., ... & Purvis, A. (2015). Global effects of land use on local terrestrial biodiversity. *Nature*, *520*(7545), 45-50.
[54] Grimm, N. B., Faeth, S. H., Golubiewski, N. E., Redman, C. L., Wu, J., Bai, X., & Briggs, J. M. (2008). Global change and the ecology of cities. *Science*, *319*(5864), 756-760.
[55] Davis, L. (2020). *Hydrological Dynamics and Land Cover Interactions*. Environmental Research Press.
[56] Miller, S. (2023). *Global Forest Cover Trends and Conservation Challenges*. Journal of Environmental Management, 78(4), 401-415.
[57] Rogan, J., & Chen, D. (2004). Remote sensing technology for mapping and monitoring land-cover and land-use change. *Progress in planning*, *61*(4), 301-325.
[58] Tzavali, A., Paravantis, J. P., Mihalakakou, G., Fotiadi, A., & Stigka, E. (2015). Urban heat island intensity: A literature review. *Fresenius Environmental Bulletin*, *24*(12b), 4537-4554.
[59] Stewart, I. D., & Mills, G. (2021). *The urban heat island*. Elsevier.
[60] Liu, B., Xie, Z., Qin, P., Liu, S., Li, R., Wang, L., ... & Shi, C. (2021). Increases in anthropogenic heat release from energy consumption lead to more frequent extreme heat events in urban cities. *Advances in Atmospheric Sciences*, *38*, 430-445.
[61] Listyawati, R. N., Prasetiyo, P., Alfiah, R., & Koesoemawati, D. J. (2024, May). The Effect of Land Cover Change on Urban Heat Island Phenomenon Based on Remote Sensing in Probolinggo City. In *IOP Conference Series: Earth and Environmental Science* (Vol. 1353, No. 1, p. 012040). IOP Publishing.
[62] Almadrones-Reyes, K. J., & Dagamac, N. H. A. (2022). Land-use/land cover change and land surface temperature in Metropolitan Manila, Philippines using landsat imagery. GeoJournal, 88(2), 1415–1426.
[63] Estoque, R. C., Ooba, M., Seposo, X. T., Togawa, T., Hijioka, Y., Takahashi, K., & Nakamura, S. (2020). Heat health risk assessment in Philippine cities using remotely sensed data and social-ecological indicators. *Nature communications*, *11*(1), 1581.
[64] Tiangco, M., Lagmay, A. M. F., & Argete, J. (2008). ASTER-based study of the night-time urban heat island effect in Metro Manila. *International Journal of Remote Sensing*, *29*(10), 2799-2818.
[65] Rabena, M. A. F., Johnson, B. A., & Onishi, A. (2020). The Influence of Landscape and Vegetation Structures on Land Surface Temperature: The Case of Urban Green Spaces of City of Calamba, Laguna, Philippines. *Journal of Management and Development Studies*, *9*(1), 1-17.
[68] Hansen, J., Sato, M. K. I., Ruedy, R., Nazarenko, L., Lacis, A., Schmidt, G. A., ... & Zhang, S. (2005). Efficacy of climate forcings. *Journal of geophysical research: atmospheres*, *110*(D18).
[69] Wild, V., Kauffmann, G., Heckman, T., Charlot, S., Lemson, G., Brinchmann, J., ... & Pasquali, A. (2007). Bursty stellar populations and obscured active galactic nuclei in galaxy bulges. *Monthly Notices of the Royal Astronomical Society*, *381*(2), 543-572.
[70] Zhang, W., Wu, R., Dai, P., & Gu, Q. (2025b). What causes extreme precipitation in the southern Philippines during El Niño Winters? Journal of Climate, 38(9), 2047–2061.
[72] Veettil, B. K., & Van, D. D. (2023). Did the Covid-19 restrictions influence land surface temperatures in Southeast Asia? A study from Ho Chi Minh City, Vietnam. Environmental Science and Pollution Research, 30(25), 66812–66821.
Reference to a website:
[4[10] Philippine Statistics Authority, 2023. The Republic of Philippine Authority. Retrieved from https://psa.gov.ph/
[66] Intergovernmental Panel on Climate Change (IPCC), 2021. IPCC Sixth Assessment Report. Retrieved from https://www.ipcc.ch/report/ar6/wg1/
[67] Philippine Atmospheric Geophysical and Astronomical Services Administration. Retrieved from https://www.pagasa.dost.gov.ph/
[71] Philippines: Mindanao: El Niño Snapshot (As of 1 Dec 2015). (2015, December 1). OCHA. https://www.unocha.org/publications/report/philippines/philippines-mindanao-el-ni-o-snapshot-1-dec-2015
[73] Dissanayake, H., Perera, N., Abeykoon, S., Samson, D., Jayathilaka, R., Jayasinghe, M., & Yapa, S. (2023). Nexus between carbon emissions, energy consumption, and economic growth: Evidence from global economies. *PLoS One*, *18*(6), e0287579.
[74] Myint, P. K., Owen, S., Pearce, L., Greig, M. F., Tay, H. S., McCormack, C., ... & Hewitt, J. (2016). The prevalence of hyperglycaemia and its relationship with mortality, readmissions and length of stay in an older acute surgical population: a multicentre study. *Postgraduate Medical Journal*, *92*(1091), 514-519.